Carbohydrate Polymers 157 (2017) 267–274

Contents lists available at ScienceDirect

Carbohydrate Polymers

journal homepage: www.elsevier.com/locate/carbpol

Synthesis and characterization of acetylated amylose and development of inclusion complexes with rifampicin

Andresa C. Ribeiro [a], Ângelo Rocha [b], Rosane M.D. Soares [c], Luís P. Fonseca [b], Nádya P. da Silveira (Dr.) (Professor) [a,*]

[a] Group of Studies of the Laboratory of Instrumentation and Molecular Dynamics (LINDIM), Chemistry Institute, Federal University of Rio Grande do Sul, 91501-970 Porto Alegre, RS, Brazil
[b] Institute for Bioengineering and Biosciences, Department of Bioengineering, Instituto Superior Técnico, Universidade de Lisboa, Av. Rovisco Pais 1, 1049-001 Lisboa, Portugal
[c] Group of Studies of the Polymeric Biomaterials (POLI-BIO), Chemistry Institute, Federal University of Rio Grande do Sul, 91501-970 Porto Alegre, RS, Brazil

ARTICLE INFO

Article history:
Received 18 June 2016
Received in revised form
17 September 2016
Accepted 20 September 2016
Available online 21 September 2016

Keywords:
Amylose
Acetylation
Rifampicin
Inclusion complexes
Drug delivery system

ABSTRACT

Amylose (AM) tends to form single helical inclusion complexes with suitable agents. These complexes are considered promising biomaterial carrier since the guest molecules can be released later, leading to many applications, especially in the pharmaceutical industry. Rifampicin (RIF) has long been recognized as an active drug against *Mycobacterium tuberculosis*, however, the administration of RIF in high dosages can originate unwanted side-effects. Due to the fact that the use of native amylose (AM) in the formation of complexes is limited by their low water solubility, it was acetylated with a medium degree of substitution (DS), allowing solubilizing (0.5 gL^{-1}) acetylated amylose (AMA) in water at neutral pH, in opposition to that observed with native amylose (trace solubility). The resulting acetylated amylose was characterized by means of Fourier Transform Infrared (FT-IR) spectroscopy and Scanning Electron Microscopy (SEM). FT-IR results indicated that the acetylation of anhydroglucose units of amylose corresponds to a low DS, whereas SEM results suggested that the smooth surfaces of amylose granules were changed into rougher surfaces after acetylation. Ultraviolet absorption spectroscopy (UV–vis) analysis confirmed the formation and allowed the quantification of both native (AM-RIF) and acetylated (AMA-RIF) amylose inclusion complexes. Their characterization in solution was performed by dynamic light scattering (DLS) and zeta potential (ZP) measurements. The average size of inclusion complexes as determined by DLS, ranged between 70 and 100 nm. Besides, ZP analysis showed that both complexes are more stable in the presence of RIF. This study may lead to the development of an effective method for the preparation of amylose inclusion complexes, which is beneficial to their further application in drug delivery systems.

1. Introduction

Amylose is a natural linear polysaccharide composed of α – 1, 4–D-glucose units (Carbinatto, Ribeiro, Colnago, Evangelista, & Cury, 2016; Luo et al., 2016; Yang et al., 2013; Zhou et al., 2016). In aqueous media, due the α-1,4 configuration, amylose can form a helical structure (Arijaje & Wang, 2015; Carbinatto et al., 2016; Zhou et al., 2016), where the hydroxyl groups are disposed on the outer surface of the helix, whereas glycosidic oxygen and methylene groups are faced to the inner core resulting in a more hydrophobic cavity, which provides binding sites with high affinity for hydrophobic ligands (Carbinatto et al., 2016). Hence, amylose can encapsulate hydrophobic guest molecules by weak intermolecular hydrophobic and van der Waals interactions, forming inclusion complexes (Luo et al., 2016).

In recent years, various bioactive molecules have been complexed with amylose for controlled release purposes (Cai, Yang, Zhang, & Wu, 2010; Carbinatto et al., 2016; Cohen, Orlova, Kovalev, Ungar, & Shimoni, 2008; Kong & Ziegler, 2014; Marinopoulou, Papastergiadis, Raphaelides, & Kontominas, 2016; Seo, Kim, & Lim, 2015; Uchino, Tozuka, Oguchi, & Yamamoto, 2002; Yang et al., 2013; Zhang et al., 2016). According to literature, amylose-guest inclusion complexes can protect these compounds during their passage through the stomach, and be released in the small intestine by the enzymatic hydrolysis of the amylose complexes (Zhang et al., 2016).

* Corresponding author at: Chemistry Institute, Universidade Federal do Rio Grande do Sul, Campus do Vale, Porto Alegre, RS, Brazil.
E-mail addresses: nadya@iq.ufrgs.br, silveira.nadya@gmail.com (N.P. da Silveira).

http://dx.doi.org/10.1016/j.carbpol.2016.09.064
0144-8617/

Rifampicin is a hydrophobic drug (He et al., 2013) that is administered with isoniazid, pyrazynamide, and ethambutol, has long been recognized as an active drug against *Mycobaterium tuberculosis* (Singh et al., 2016). Conventional therapy against tuberculosis (TB) involves prolonged oral administration of high systemic doses of single or combined antibiotics, which often causes unwanted side-effects by high systemic exposure (Singh et al., 2015), such as hepatotoxicity, fever, gastrointestinal disturbance, immunological reaction (He et al., 2013), failure of treatment, which leads to development of multidrug- resistant TB (Singh et al., 2016). Over the past decades, various types of delivery systems have been prepared (He et al., 2013; Hu, Feng, & Zhu, 2012; Manca et al., 2012; Tewes, Brillault, Couet, & Olivier, 2008; Zaru et al., 2009). However, these systems present some disadvantages such as inconvenient route of administration, manufacturing complexity and uncertain safety (He et al., 2013).

Amylose is of particular interest in the design of biomedical applications (Carbinatto et al., 2016; Marinopoulou et al., 2016). Although the amylose-guest inclusion complexes have been extensively studied, inclusion complexes with RIF were not tested or published in the literature according to our knowledge. Thus, this study contributes for a better understanding on the nature and functional properties of these amylose complexes, provides a potential novelty for inclusion of RIF, and shows an easy methodology for the production of these drug delivery systems.

The use of native amylose for certain applications is limited by their specific physical properties (Kida, Minabe, Okabe, & Akashi, 2007; Wulff, Steinert, & Höller, 1998; Zhou et al., 2016). Firstly, this polysaccharide has low water solubility due to the multiple hydrogen bonds between the amylose hydroxyl groups (Kida et al., 2007). Furthermore, amylose has strong tendency to retrograde (Kida et al., 2007; Wulff et al., 1998). These properties can limit the movement of the helices of amylose molecules, which brings difficulties to the preparation of amylose-guest inclusion complexes in aqueous solution (Zhou et al., 2016).

As reported in previous studies (Arijaje & Wang, 2015; Arijaje, Wang, Shinn, Shah, & Proctor, 2014; Wulff et al., 1998; Zhou et al., 2016), chemical modification is a common way used to change properties of starch and amylose. Wulff et al. (1998) and Arijaje et. al, Arijaje and Wang (2015) found out that acetylation significantly increased the amount of soluble amylose complexes recovered from aqueous solution as well as enhanced the inclusion of oleic acid.

The appropriate chemical modification of hydroxyl groups of anhydroglucose units of amylose such as through the introduction of acetyl groups allows weaken the multiple hydrogen bonds of amylose without significant loss of the helical structure. This modification results in acetylated amylose which presents higher solubility in aqueous media as well as a much weaker retrograde tendency in relation to the native amylose (Kida et al., 2007; Zhou et al., 2016). However, according to our knowledge on the formation of inclusion complexes and inclusion capacity of the acetylated amylose is limited and has not been clearly reported.

In this work, acetylated amylose with a low degree of substitution was prepared and the physicochemical properties were subsequently investigated by UV–vis, Fourier transform infrared (FT-IR) and scanning electron microscopy (SEM). Afterwards, the potential of acetylated amylose for the production inclusion complexes was explored. For this, an aqueous dispersion of RIF with native or acetylated amylose was used and tested for formation of potential inclusion amylose complexes. The RIF inclusion complexes were prepared and characterized by analyzes of yield, content of complexed drug, dynamic light scattering (DLS) and zeta potential (ZP).

2. Materials and methods

2.1. Materials

Amylose (AM) from potato (average $M_w > 150{,}000$) and rifampicin were purchased from Sigma Aldrich® and used without any further purification. Potassium hydroxide and acetic anhydride of analytical of grade were also obtained from Sigma Aldrich. All other chemical reagents were of analytical grade and used as received.

2.2. Preparation of acetylated amylose

Acetylated amylose (AMA) was prepared according to the method proposed by Mark and Mehltretter (1972). The experimental procedure used in this work follows a similar experimental condition used by these authors that obtained also a lower degree of substitution of native amylose (Wulff et al., 1998) or starch (Mark & Mehltretter, 1972). First, amylose was dried at 50 °C for 12 h, then 1 g of amylose and 3 mL acetic anhydride were mixed in a glass vial and the solution was stirred on a magnetic stirrer 500 rpm for 5 min. Afterwards, 0.9 mL of 50% NaOH aqueous solution were added under continuous stirring. The mixture was stirred for more 90 min at 90 °C. Then, the suspension was cooled to 50 °C and then amylose precipitated with the addition of 10 mL of 96% ethanol. At once, the solution was centrifuged at 3000 rpm for 10 min (Labofuge 200, Heraeus Instruments) and then the precipitated was washed with 96% ethanol and centrifuged two times till most of acetic anhydride was eliminated. Finally, precipitated obtained was dried for 12 h in vacuum pump at 2×10^{-2} mbar (rotary vane pump RZ 2.5, Vacuubrand) at 25 °C.

2.3. Preparation of amylose-rifampicin (AM-RIF) and acetylated amylose-rifampicin (AMA-RIF) inclusion complexes

Amylose-rifampicin complexes were prepared with 10 mg of amylose dissolved in 20 mL of 0.1 M KOH solution, *i.e.*, 0.5 gL^{-1}. The solution was stirred on a magnetic stirrer for 6 h at 90 °C under a nitrogen atmosphere. RIF solution (0.05 gL^{-1}) was prepared separately by dissolving in H_2O. After amylose dissolution, the solution pH was adjusted to 7.0 with 0.2 M HCl and then a rifampicin aqueous solution was added (Cohen et al., 2008).

The inclusion complex of acetylated amylose and rifampicin was prepared according to similar procedure as described above except that acetylated amylose was directly solubilized in water at neutral pH (0.5 gL^{-1}) and then mixed with rifampicin aqueous solution (0.05 gL^{-1}). Both solutions were mixed at 40 °C and then stirred for 24 h at 65 °C. All experiments were performed in triplicate.

2.4. Characterization of the acetylated amylose

2.4.1. Determination of acetylation and degree of substitution

The percentage of acetylation (%A_c) and degree of substitution (DS) were determined by titration using the method suggested by Wurzburg (1964) with the following modifications. The powder of AMA (0.1 g) was weighed in a glass vial and 5 mL of 75% ethanol was added. The slurry was stirred and warmed to 50 °C for 30 min. Afterwards, 4 mL of aqueous solution of potassium hydroxide (0.2 M) was added and the solution was stirred for more 1 h. The excess of alkaline was titrated with 0.2 N hydrochloride acid using phenolphthalein as indicator. A blank, using the original unmodified amylose, was also used as control. The experiment was performed in duplicate.

Acetyl content (%A_c) was calculated according to Eq. (1) and then the degree of substitution (DS) value was calculated by Eq. (2).

$$\%Ac = \frac{\left[\left(\frac{(v_2 - v_1)}{1000\text{mL}}\right) \times \text{Molarity HCl} \times 43 \times 100\right]}{m_{sample}\,(g)} \quad (1)$$

$$DS = \frac{(162\ x\ \%Ac)}{[43 \times 100 - (42\ x\ \%Ac)]} \quad (2)$$

where:

v_1 and v_2: volume (mL) of HCl used in the titration of blank and in sample, respectively;

m_{sample}: sample amount as dry product (g);

43: molecular weight of acetyl group;

162: molecular weight of anhydroglucose unit;

42: molecular weight of acetyl group minus the atomic weight of hydrogen atom.

The relationship between these two factors (%Ac and DS) is described and dependent of the mathematical relation given by the Eqs. (1) and (2).

2.4.2. Attenuated total reflectance fourier transform infrared spectroscopy (ATR-FT-IR)

Native and acetylated amylose were characterized using Perkin-Elmer Spectrum 400 FT-IR/FT-NIR spectrometer equipped with an attenuated total reflection (ATR) accessory. The spectral regions were recorded at a resolution of 4 cm^{-1}, 32 scans, and wavelength range was between 600 and 4000 cm^{-1}. Amylose samples were placed on the ATR crystal for analysis, at room temperature (25 ± 0.1 °C). All experiments were performed in triplicate.

2.4.3. Scanning electron microscopy (SEM)

The surface morphologies of native and acetylated amylose were examined by FE-SEM Instrument (Gemini 1530, Zeiss, Germany). Solid samples were deposited on a carbon tape and sputtered with a Pt-layer (Sputter Coater 208HR, Cressington, UK). Pictures were taken at an excitation voltage of 7.0 kV.

2.5. Characterization of the inclusion complexes

2.5.1. UV spectroscopy analysis, efficiency and loading capacity of inclusion complexes

Complex formation between native or acetylated amylose with rifampicin, were studied by spectroscopic method. The UV spectra were obtained on a PerkinElmer spectrophotometer 554 using a quartz cell with optical length of 1 cm. For each spectrum, covering the 200–700 nm wavelength range, a baseline was established, by placing in the reference compartment native amylose or acetylated amylose at the same concentration of the samples.

Besides this, the spectroscopic technique was also used to determine the inclusion efficiency (%IE) and loading capacity (%LC) of RIF in the inclusion complexes. For this, absorbance of various RIF concentrations was recorded over wavelengths ranging from 200–700 nm. The maximum peak with minimum interference was centered at 472 nm which allows obtain a calibration curve using a linear regression which indicate the RIF concentrations in the respective solution. Complexes were also prepared and free RIF concentration was determined in the same manner. From that, the percentage of included RIF and loading capacity were determined (Eqs. (3) and (4)).

$$\%IE = \frac{\text{Quantity of RIF in the complex}}{\text{Total quantity of RIF}} \times 100 \quad (3)$$

$$\%LC = \frac{\text{Quantity of RIF in the complex}}{\text{Total quantity of amylose}} \times 100 \quad (4)$$

All measurements were carried out at 25.0 ± 0.1 °C. All data shown represent the average of, at least, three independent determinations.

2.5.2. Particle size analysis (DLS)

The apparent average hydrodynamic radii (R_h) of inclusion complexes were performed by dynamic light scattering (DLS) using a Zetasizer Nano ZS (Malvern Instruments, USA) equipped with a 4 mW He-Ne laser. Measurements were performed at a wavelength of 632.8 nm, using the detection angle of 173°, at 25 ± 0.1 °C. All samples were purified by passing through a 0.45-μm filter (PTFE, Millex Millipore) and each sample was measured 3 times. The reported values are the mean diameter ± s.d.

2.5.3. Zeta potential (ZP)

The ZP was measured by a Malvern Zetasizer (Malvern Instruments, USA) at 25 ± 0.1 °C. ZP was calculated using the Smoluchowski equation from the electrophoresis mobility and electric field strength. The value was recorded as the average of five measurements and the values reported are the mean ± s.d.

3. Results and discussion

3.1. Acetyl content (%A_c), degree of substitution (DS) and FT-IR results of acetylated amylose

The physical properties of the acetylated starch are determined by the degree of substitution (DS) (Colussi et al., 2015; Golachowski et al., 2015). DS indicates the average number of hydroxyl groups substituted per anhydroglucose unit (Sun et al., 2016). As each anhydroglucose unit has three hydroxyl groups (OH-2, OH-3 and OH-6) available for substitution, the maximum possible DS is 3 (Han, Gao, Liu, Huang, & Zhang, 2013; Sun et al., 2016). According to literature acetylated anhydroglucose units with high DS are practically insoluble in water in opposition with acetylated anhydroglucose units with low DS, which are characterized by higher solubility in water (Golachowski et al., 2015).

In this study, the results revealed that the DS displayed for acetylated amylose was low (0.86 ± 0.01) (Table 1) which corresponds to a substitution of about 22% of total OH groups available per anhydroglucose unit. For this low DS, the acetylated amylose presents higher solubility (0.5 gL^{-1}) in water at neutral pH than native amylose (trace) (Table 1). The modification maybe occurs essentially in the outside chains, while the chains inside were not involved in substitution at all.

Table 1
Acetyl content (% Ac) and degree substitution (DS) of native and acetylated amylose.

Sample	% Ac	DS	Solubility in water at neutral pH (gL^{-1})
Native	0	0	Trace
Acetylated	Serie 1: 18.9	Serie 1: 0.87	Soluble
	Serie 2: 18.5	Serie 2: 0.85	Soluble
	Serie 3: 16.8	Serie 3: 0.76	Soluble
Average*	18.7 ± 0.7	0.86 ± 0.03	

* The results are the mean of three determinations ($p < 0.05$).

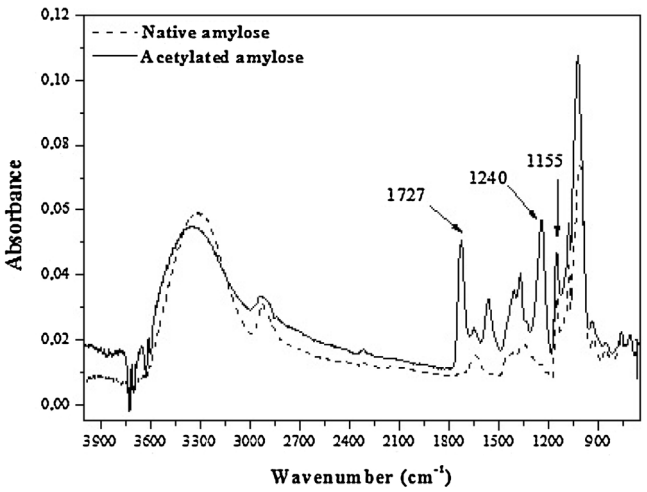

Fig. 1. FT-IR spectra of (----) native amylose and (—) acetylated amylose.

The structural changes caused by introduction of acetyl groups into amylose structure, were also verified and confirmed by FT-IR analysis (Fig. 1).

In comparison to the spectrum of native amylose, new peaks at 1240 cm^{-1} (due C—O stretch vibration) and 1727 cm^{-1} (due to C=O group), appeared in the spectrum of acetylated amylose (Colussi et al., 2015; Kulkarni, Sinha, & Kumar, 2015). These peaks are attributed to the absorbance of the ester carbonyl of the acetyl moiety (Colussi et al., 2015) and it is an indicative that the acetyl groups were covalently bound to the anhydroglucose unit. Furthermore, a band with peak at 1155 cm^{-1} indicates the formation of amylose acetate (Kulkarni et al., 2015).

On the other hand, peaks in the region 1850–1760 cm^{-1} and 1700 cm^{-1} are attributed to acetic anhydride (Colussi et al., 2015; Kulkarni et al., 2015) and acetic acid (Colussi et al., 2015), respectively. In this study, the FT-IR spectrum (Fig. 1) shows the absence of these peaks in special at 1850 cm^{-1}. This fact is an indicative that the product obtained after acetylation of native amylose was free of unreacted acetic anhydride and acetic acid.

Finally, a shift in the adsorptions corresponding to stretching vibrations of hydroxyl groups (3000–3600 cm^{-1}) and a decrease in the adsorptions of bending vibrations (1650 cm^{-1}) are due to the introduction of acetyl groups in the amylose (Halal et al., 2015). In this study changes in these absorptions also were observed (Fig. 1) and this fact confirms that the amylose acetylation was successfully achieved.

3.2. Analysis of morphology of acetylated amylose

The morphology of native and acetylated amylose granules were investigated using scanning electron microscopy (SEM) (Fig. 2). The native amylose granules are essentially spherical with smooth surfaces while after acetylation small irregular particles with rough surfaces (Fig. 2) can be observed. SEM images show that acetylated amylose granules suffer external surface modification probably associated with its higher solubility in water at neutral pH, when compared to the native amylose. In spite of the surface modification, spherical structures can be observed (Fig. 2c and d). It seems that acetylation may occur essentially in the outside chains of the amylose granules, whereas the chains inside were not involved.

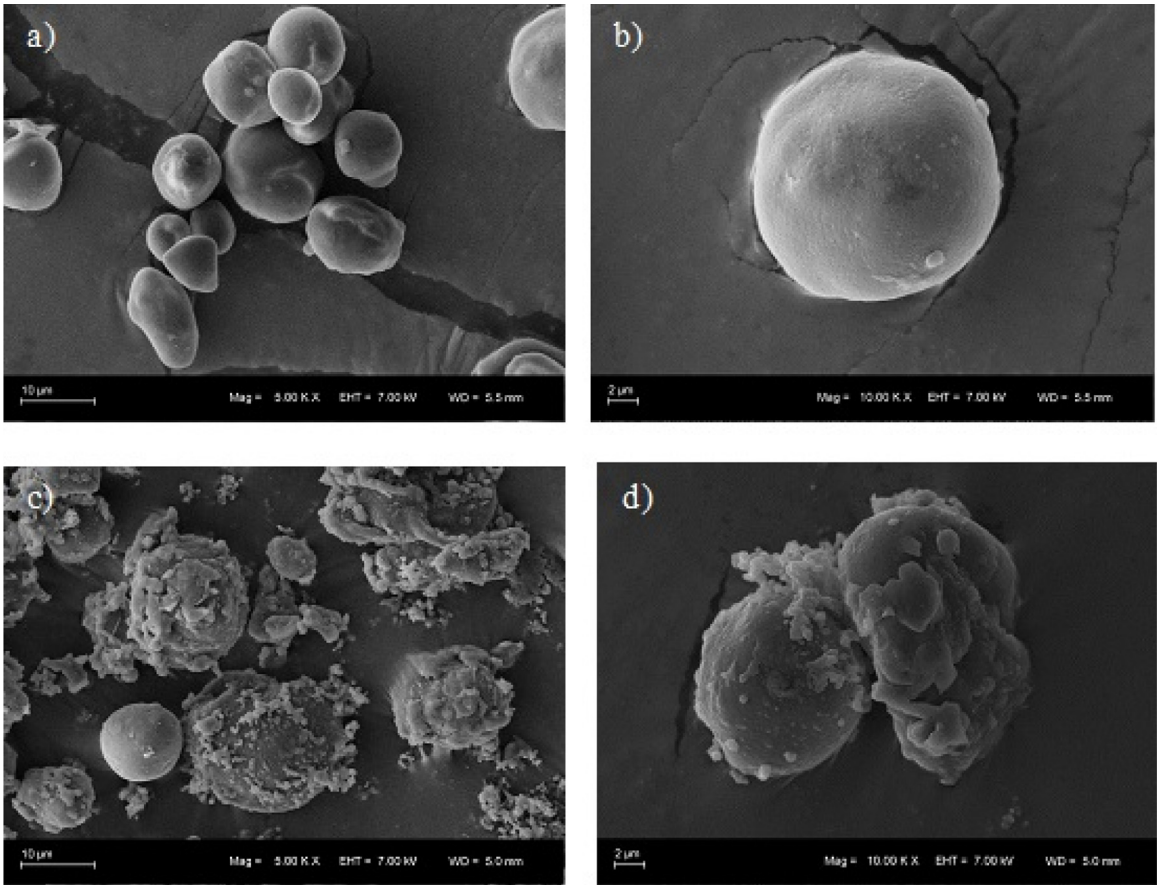

Fig. 2. SEM micrographs of (a) and (b) native amylose, (c) and (d) acetylated amylose.

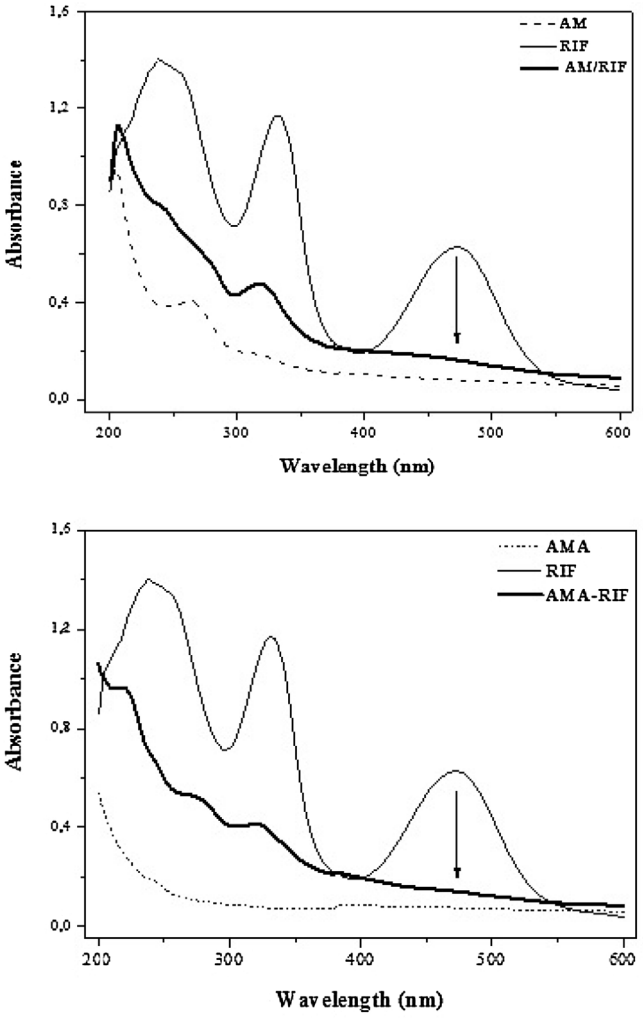

Fig. 3. UV–vis spectrum of native amylose (AM), rifampicin (RIF), and AM-RIF complex (on top) and acetylated amylose (AMA), rifampicin (RIF), and AMA-RIF complex at 65 °C (on the bottom).

According to literature (Teodoro, Mali, Romero, & de Carvalho, 2015) the aggregation of amylose granules after acetylation could be attributed to the introduction of hydrophilic groups to the amylose molecules, which resulted in increase of intermolecular hydrogen bonds in aqueous solutions.

3.3. Analysis of UV–vis spectrum of native and acetylated amylose, RIF and inclusion complexes

UV absorption spectroscopy is an effective method to explore the formation of inclusion complexes (Kaur, Uppal, Kaur, Agarwal, & Mehta, 2015). Besides that, this technique is helpful to show and determine the content of guest molecules in the inclusion complexes (Zhou et al., 2016). For RIF solution in water the UV–vis absorbance spectra show two bands typically at 333 nm and 472 nm. These bands disappear or decrease significantly in the spectrum after complexation of RIF with native and acetylated amylose. The native (AM) and acetylated amylose (AMA) solutions do not contribute significantly in the UV–vis absorption spectra range of RIF specifically at 472 nm (Fig. 3). For this reason, the formation of the RIF-complex in solution was investigated by UV–vis measurements in these studies (Fig. 3). Thus, spectral changes and absorbance decrease, specifically at this wavelength can be directly related to lower concentrations of RIF in solution, due to its partial inclusion in the amylose complexes.

Table 2
Inclusion efficiency (%IE) and loading capacity (%LC) of RIF included into AM and AMA hydrophobic cavities at 40 °C and 65 °C.

Sample	% IE—40 °C	% IE—65 °C	% LC—40 °C	% LC—65 °C
AM-RIF	70.9 ± 0.9	78.3 ± 2.2	7.04 ± 0.1	7.85 ± 0.1
AMA-RIF	79.5 ± 4.5	89.1 ± 1.6	7.97 ± 0.3	8.93 ± 0.1

Furthermore, as the inclusion complexes formation causes changes in the absorption spectrum of a guest molecule, change in the color of the solution can occur (Niamnont, Promchat, Siangma, Pramaulpornsatit, & Sukwattanasinitt, 2015). In this study a decreased in the absorbance at 472 nm was also notice by loss of the characteristic orange/yellow color of RIF after guest molecule complexation (Fig. 4).

These observed color changes might be due to the perturbation of the chromophore electrons of the RIF after its inclusion into the hydrophobic cavity of amylose structure. Therefore, UV–vis spectrum confirmed the formation of the complexes and can be used to determine the inclusion efficiency and loading capacity through the content of guest molecules in the inclusion complexes.

Inclusion efficiency and loading capacity are quantitative parameters that illustrate the amount of included RIF in the complex of native amylose (AM-RIF) and acetylated amylose (AMA-RIF). These parameters were determined by the variation of the absorbance values at 472 nm is the linear regression of the calibration curve. Overall, these data suggest that the inclusion efficiency and loading capacity are dependent of the amylose molecule structure, and of temperature used during the RIF inclusion complexes formation (Table 2).

The increase of reaction temperature from 40 to 65 °C used during the complex formation enhances about 10% and 1% the inclusion efficiency and loading capacity, respectively for both types of amylose. This result was attributed to increased amylose chain mobility at higher temperature. This increased in mobility of the amylose structure promoted higher physical contact between amylose and RIF molecules which improves the formation of inclusion complexes. This hypothesis is in agreement with previous studies on amylose inclusion complexes with fatty acids (Luo et al., 2016; Seo et al., 2015)

On the other hand, the RIF – inclusion complexes prepared with AMA presented higher values of the inclusion efficiency (about 10%) and loading capacity (about 1%) independent of the temperature used during the formation of inclusion complexes. The increase in the% IE and% LC are related to the substitution of hydroxyl by acetyl group that promote better interaction with rifampicin ionization groups enhancing RIF inclusion in acetylated amylose.

According to literature, the charge of the guest molecule is an important parameter that influences the efficiency of complexation (Anshakova et al., 2015). Additionally, it is also known that, for example, non-polar interactions between amylose and the hydrophobic portion of the guest molecule is a driving force for the complex formation (Kim & Huber, 2016; Lii, Stobinski, Tomasik, & Liao, 2003). Therefore, it is important to know the structure of guest molecules such as RIF for better understanding of its interactions with amylose chains.

The RIF molecule (Scheme 1), contains several ionized groups with pKa in the ranges of pH 1 and 11. Among these groups there are two mainly important, the hydroxyl in C4 and the 3′-piperazin nitrogen, with pKa of 1.7 and 7.9, respectively (Tewes et al., 2008). Between pH 1.7 and 7.9 the ionic species are a globally neutral zwitterionic form (Ferreira et al., 2015; Tewes et al., 2008).

In studies for inclusion complexes between RIF and cyclodextrin, it was demonstrated that the interactions, at neutral pH, are

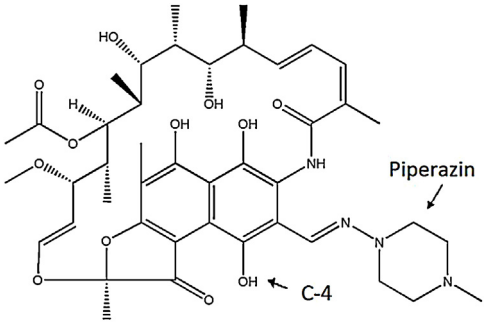

Scheme 1. RIF chemical structure, the hydroxyl group in C-4 and the 3′-piperazin nitrogen group.

mediated through the piperazine group. The calculation of the minimization energy for formation of inclusion complexes indicated that the most stable complex has the rifampicin complexed through the piperazine tail enclosed into the hydrophobic cavity of cyclodextrin (Chadha et al., 2010; Ferreira, Ferreira, Vizzotto, Federman Neto, & de Oliveira, 2004). For this reason, with this work there is a good hypothesis that the acetyl groups of the AMA can have promoted the preference of piperazine tail enclosed into the hydrophobic cavity of amylose helix too.

This fact may be ascribed to the alignment of acetyl groups toward the cavity, increasing the interaction of guest molecule and hydrophobic cavity and consequently explain the higher values of% IE and% LC of RIF obtained for acetylated amylose in this work. This hypothesis is in great agreement with proposed in other study on inclusion complexes between acetylated starch and stearic acid (Arijaje et al., 2014).

The other hypothesis to explain the lower values of% IE and% LC obtained with AM-RIF complexes in this work is due to the alkaline environment used for native amylose dissolution. After native amylose dissolution the pH was adjusted to 7.0 with HCl increasing significantly the ionic strength. The ions present in this solution with higher ionic strength can compete directly with the piperazin, the ionizable group of the RIF that interact with the ionic groups of the amylose and decreases the concentration of the antibiotic nearby of the amylose molecule structure. This competition affects negatively the complexes formation and inclusion of RIF in the hydrophobic cavity through the piperazin tail. This can be one possible reason responsible for the lower inclusion efficiency and loading capacity of complexes prepared from native amylose observed in this work.

3.4. Particle size and zeta potential analysis of the inclusion complexes

The efficient function of drug delivery systems is influenced by particle size, surface charge, surface modification, and hydrophobicity (Kumari, Yadav, & Yadav, 2010). Thus, the knowledge of these properties is important for a better understanding of the applicability of these complexes in *in vivo* systems. In this study, suspensions produced by the complexation of RIF with native and acetylated amylose were analyzed obtaining the average size (d_h), polydispersity index (PdI) and zeta potential (ZP) values. They are reported in Table 3 and represent the average of three measurements.

Table 3
Mean particle size (d_h, n = 3), polydispersity index (PdI) and zeta potential (ZP) of native and acetylated amylose and RIF inclusion complexes.

Sample[a]	d_h (nm) (±SD)	PdI (±SD)	ZP (mV) (±SD)
AM	74.3 ± 2.0	0.42 ± 0.1	−9.1 ± 1.0
AM-RIF—65 °C	117.1 ± 2.0	0.33 ± 0.1	−15.7 ± 1.2
AMA	78.9 ± 4.0	0.56 ± 0.0	−3.6 ± 1.0
AMA-RIF—65 °C	75.8± 2.0	0.42 ± 0.1	−8.0 ± 1.3

[a] n = 3.

The size and charge are important parameters for characterization of drug delivery systems as they determine the interaction of the inclusion complexes with the cell membrane and their penetration across the physiological drug barriers (Kumari et al., 2010). For *in vivo* applications, for example, polymeric nanoparticles should have intermediate size (20–100 nm). In this range of size, when they are designed appropriately, nanoparticles can circulate in the blood for long periods of time (Elsabahy & Wooley, 2012). The average size of inclusion complexes formulated in this study ranged between 70 and 100 nm, indicating that the inclusion complexes developed can be used as drug delivery systems.

For native amylose, without the guest molecules, the particle size was (74.3 ± 2.0) nm and its relative average PdI was 0.42 ± 0.1. This size increased to (117.1 ± 2.0) nm, with a polydispersity index of 0.33 ± 0.1, when RIF was incorporated in the AM-RIF inclusion complex.

For AMA, the average size was (78.9 ± 4.0) nm with a relative average polydispersity index of 0.56 ± 0.0. Additionally, as the size of the amylose grains (d_h) only increases slightly from 74.3 to 78.9 nm for native and acetylated amylose molecules, respectively, and the difference it is inside of the experimental error, it is possible to assume that the slightly change in the helicity of the acetylated amylose molecules is not significant.

Complexes of AMA-RIF presented a similar size of AMA (d_h: 75.8 ± 2.0; PdI: 0.42 ± 0.1). These results suggest that for these inclusion complexes, because of AMA contains acetyl groups, stronger hydrophobic interactions with the piperazine tail of RIF molecule are induced (Kaur, Mehta, Kumar, Bhanjana, & Dilbaghi, 2015) and AMA-RIF tends to close slightly under itself in comparison with increase of about 40% in size observed for AM-RIF complexes.

Zeta potential (ZP) is a characteristic directly related with the stability of the inclusion complexes (Doostmohammadi et al., 2011). Studies indicated that ZP with values of ± 30 mV is a feature of drug delivery systems with good stability in suspension (Do, Pai, Rizvi, & D'Souza, 2010; Silveira et al., 2016). However, ZP also has important biological effects *in vivo* (Doostmohammadi et al., 2011) and low ZP values have longer blood circulation times

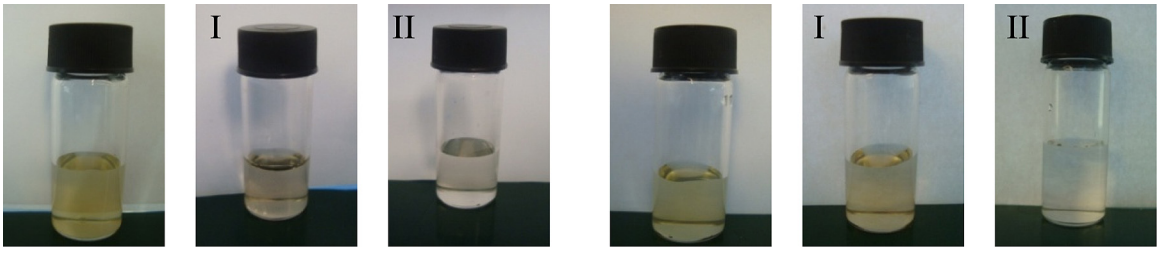

Fig. 4. Loss of orange/yellow color of RIF after complexation at (I) 40 °C and (II) 65 °C in: (left) native amylose (AM) and (right) acetylated amylose (AMA).

than charged particles (Booysen et al., 2013). Additionally, other studies have shown that material with a negative zeta potential is more accessible for the attachment than uncharged surfaces or even with positive electric charge (Booysen et al., 2013; Do et al., 2010; Doostmohammadi et al., 2011; Silveira et al., 2016). Positively charged particles, for example, have a strong electrostatic interaction with intestinal mucosa (negatively charged). This fact may slow down the progression and penetration of these particles to the epithelial cell surface, reducing their uptake (Booysen et al., 2013; Minimol, Paul, & Sharma, 2013).

In this study, ZP values remained in the range of negative values for all complexes and vary between −3.6 mV and −15.7 mV (Table 3). These negative values could be attributed to the presence of hydroxyl groups of amylose molecules onto the surface of the complexes. As it is known, the amylose is made of glucose units, and the hydroxyl glucose residues have a high pK_a (12.35) (Gonçalves & Gama, 2008) and for this reason the inclusion complexes developed in this work have a poorly ionized surface at neutral pH.

Besides this, our results suggest that AM is more stable than AMA (ZP of AM is -9.1 ± 1.0 mV and ZP of AMA is -3.6 ± 1.0 mV) due to AM having a higher amount of hydroxyl group in the helix outer surface than the AMA.

Finally, the inclusion of RIF improved a colloidal stability in both complexes (ZP values decreased to -15.7 ± 1.2 mV in the AM and to -8.0 ± 1.3 mV in the AMA). The increase in colloidal stability could be due to negative charge added by the RIF molecules when loaded into the inclusion complexes.

4. Conclusions

In conclusion, acetyl groups were introduced into the structure of amylose, which was confirmed by FT-IR. SEM data indicated that the amylose surface was modified and their surface became rougher after acetylation. The results of UV spectroscopy, DLS and ZP analysis confirmed the formation of the AM-RIF and AMA-RIF inclusion complexes. The results demonstrated that it is possible to develop inclusion complexes of RIF with AM and AMA with moderate efficiency. Finally, the complexes formed have adequate size for *in vivo* applications, and the lower ZP values are important for complexes to have longer blood circulation time and be more accessible for the attachment in the epithelial cell surface, which increase their uptake. Thus, this study may lead to the development of an effective and innovative method of drug delivery through inclusion of RIF in amylose complexes and eventual use against *tuberculosis*.

Acknowledgments

The authors thank CAPES (Coordenação de Aperfeiçoamento de Pessoal de Nível Superior) and CNPq (Conselho Nacional de Desenvolvimento Científico e Tecnológico) for their financial support. Ângelo Rocha is grateful for financial support from Fundação para a Ciência e Tecnologia (FCT) through a Ph.D. grant (SFRH/BD/93049/2013).

References

Anshakova, A. V., Yermolenko, Y. V., Konyukhov, V. Y., Polshakov, V. I., Maksimenko, O. O., & Gelperina, S. E. (2015). Intermolecular interactions in rifabutin—2-Hydroxypropyl-β-cyclodextrin—Water solutions. *Russian Journal of Physical Chemistry A*, *89*(5), 797–801.

Arijaje, E. O., & Wang, Y.-J. (2015). Effects of chemical and enzymatic modifications on starch–oleic acid complex formation. *Journal of Agricultural and Food Chemistry*, *63*(16), 4202–4210.

Arijaje, E. O., Wang, Y.-J., Shinn, S., Shah, U., & Proctor, A. (2014). Effects of chemical and enzymatic modifications on starch–stearic acid complex formation. *Journal of Agricultural and Food Chemistry*, *62*(13), 2963–2972.

Booysen, L., Kalombo, L., Brooks, E., Hansen, R., Gilliland, J., Gruppo, V., & Kotze, A. F. (2013). In vivo/in vitro pharmacokinetic and pharmacodynamic study of spray-dried poly-(dl-lactic-*co*-glycolic) acid nanoparticles encapsulating rifampicin and isoniazid. *International Journal of Pharmaceutics*, *444*(1), 10–17.

Cai, X., Yang, L., Zhang, L.-M., & Wu, Q. (2010). Evaluation of amylose used as a drug delivery carrier. *Carbohydrate Research*, *345*(7), 922–928.

Carbinatto, F. M., Ribeiro, T. S., Colnago, L. A., Evangelista, R. C., & Cury, B. S. F. (2016). Preparation and characterization of amylose inclusion complexes for drug delivery applications. *Journal of Pharmaceutical Sciences*, *105*(1), 231–241.

Chadha, R., Saini, A., Gupta, S., Arora, P., Thakur, D., & Jain, D. V. S. (2010). Encapsulation of rifampicin by natural and modified β-cyclodextrins: Characterization and thermodynamic parameters. *Journal of Inclusion Phenomena and Macrocyclic Chemistry*, *67*(1–2), 109–116.

Cohen, R., Orlova, Y., Kovalev, M., Ungar, Y., & Shimoni, E. (2008). Structural and functional properties of amylose complexes with genistein. *Journal of Agricultural and Food Chemistry*, *56*(11), 4212–4218.

Colussi, R., El Halal, S. L. M., Pinto, V. Z., Bartz, J., Gutkoski, L. C., da Rosa Zavareze, E., & Dias, A. R. G. (2015). Acetylation of rice starch in an aqueous medium for use in food. *LWT Food Science and Technology*, *62*(2), 1076–1082.

Do, D. P., Pai, S. B., Rizvi, S. A. A., & D'Souza, M. J. (2010). Development of sulforaphane-encapsulated microspheres for cancer epigenetic therapy. *International Journal of Pharmaceutics*, *386*(1–2), 114–121.

Doostmohammadi, A., Monshi, A., Salehi, R., Fathi, M. H., Golniya, Z., & Daniels, A. U. (2011). Bioactive glass nanoparticles with negative zeta potential. *Ceramics International*, *37*(7), 2311–2316.

Elsabahy, M., & Wooley, K. L. (2012). Design of polymeric nanoparticles for biomedical delivery applications. *Chemical Society Reviews*, *41*(7), 2545–2561.

Ferreira, D. A., Ferreira, A. G., Vizzotto, L., Federman Neto, A., & de Oliveira, A. Gomes. (2004). Analysis of the molecular association of rifampicin with hydroxypropyl-β-cyclodextrin. *Revista Brasileira de Ciências Farmacêuticas*, *40*(1), 43–51.

Ferreira, Q. S., Silva, S. W., Santos, C. M. B., Ribeiro, G. C., Guilherme, L. R., & Morais, P. C. (2015). Rifampicin adsorbed onto magnetite nanoparticle: SERS study and insight on the molecular arrangement and light effect. *Journal of Raman Spectroscopy*, *46*(9), 765–771.

Golachowski, A., Zięba, T., Kapelko-Żeberska, M., Drożdż, W., Gryszkin, A., & Grzechac, M. (2015). Current research addressing starch acetylation. *Food Chemistry*, *176*, 350–356.

Gonçalves, C., & Gama, F. M. (2008). Characterization of the self-assembly process of hydrophobically modified dextrin. *European Polymer Journal*, *44*(11), 3529–3534.

Halal, S. L. M. E., Colussi, R., Pinto, V. Z., Bartz, J., Radunz, M., Carreño, N. L. V., & Zavareze, E. d. R. (2015). Structure, morphology and functionality of acetylated and oxidised barley starches. *Food Chemistry*, *168*, 247–256.

Han, F., Gao, C., Liu, M., Huang, F., & Zhang, B. (2013). Synthesis, optimization and characterization of acetylated corn starch with the high degree of substitution. *International Journal of Biological Macromolecules*, *59*, 372–376.

He, D., Deng, P., Yang, L., Tan, Q., Liu, J., Yang, M., & Zhang, J. (2013). Molecular encapsulation of rifampicin as an inclusion complex of hydroxypropyl-β-cyclodextrin: Design; characterization and in vitro dissolution. *Colloids and Surfaces B: Biointerfaces*, *103*(0), 580–585.

Hu, C., Feng, H., & Zhu, C. (2012). Preparation and characterization of rifampicin-PLGA microspheres/sodium alginate in situ gel combination delivery system. *Colloids and Surfaces B: Biointerfaces*, *95*, 162–169.

Kaur, G., Mehta, S. K., Kumar, S., Bhanjana, G., & Dilbaghi, N. (2015). Coencapsulation of hydrophobic and hydrophilic antituberculosis drugs in synergistic Brij 96 microemulsions: A biophysical characterization. *Journal of Pharmaceutical Sciences*, *104*(7), 2203–2212.

Kaur, K., Uppal, S., Kaur, R., Agarwal, J., & Mehta, S. K. (2015). Energy efficient, facile and cost effective methodology for formation of an inclusion complex of resveratrol with hp-β-CD. *New Journal of Chemistry*, *39*, 8855–8865.

Kida, T., Minabe, T., Okabe, S., & Akashi, M. (2007). Partially-methylated amyloses as effective hosts for inclusion complex formation with polymeric guests. *Chemical Communications*, *15*, 1559–1561.

Kim, J.-Y., & Huber, K. C. (2016). Preparation and characterization of corn starch-β-carotene composites. *Carbohydrate Polymers*, *136*, 394–401.

Kong, L., & Ziegler, G. R. (2014). Molecular encapsulation of ascorbyl palmitate in preformed V-type starch and amylose. *Carbohydrate Polymers*, *111*, 256–263.

Kulkarni, S. D., Sinha, B. N., & Kumar, K. J. (2015). Physicochemical and drug release characteristics of acetylated starches of five Lagenaria siceraria cultivars. *International Journal of Biological Macromolecules*, *72*, 1005–1012.

Kumari, A., Yadav, S. K., & Yadav, S. C. (2010). Biodegradable polymeric nanoparticles based drug delivery systems. *Colloids and Surfaces B: Biointerfaces*, *75*(1), 1–18.

Lii, C.-y., Stobinski, L., Tomasik, P., & Liao, C.-d. (2003). Single-walled carbon nanotube—Potato amylose complex. *Carbohydrate Polymers*, *51*(1), 93–98.

Luo, Z., Zou, J., Chen, H., Cheng, W., Fu, X., & Xiao, Z. (2016). Synthesis and characterization of amylose—Zinc inclusion complexes. *Carbohydrate Polymers*, *137*, 314–320.

Manca, M. L., Manconi, M., Valenti, D., Lai, F., Loy, G., Matricardi, P., & Fadda, A. M. (2012). Liposomes coated with chitosan—Xanthan gum (chitosomes) as potential carriers for pulmonary delivery of rifampicin. *Journal of Pharmaceutical Sciences*, *101*(2), 566–575.

Marinopoulou, A., Papastergiadis, E., Raphaelides, S. N., & Kontominas, M. G. (2016). Morphological characteristics, oxidative stability and enzymic hydrolysis of amylose-fatty acid complexes. *Carbohydrate Polymers*, *141*, 106–115.

Mark, A. M., & Mehltretter, C. L. (1972). Facile preparation of starch triacetates. *Starch Stärke*, *24*(3), 73–76.

Minimol, P. F., Paul, W., & Sharma, C. P. (2013). PEGylated starch acetate nanoparticles and its potential use for oral insulin delivery. *Carbohydrate Polymers*, *95*(1), 1–8.
Niamnont, N., Promchat, A., Siangma, C., Pramaulpornsatit, C., & Sukwattanasinitt, M. (2015). A novel phenylacetylene-indolium fluorophore for detection of cyanide by the naked eye. *RSC Advances*, *5*(79), 64763–64768.
Seo, T.-R., Kim, J.-Y., & Lim, S.-T. (2015). Preparation and characterization of crystalline complexes between amylose and C18 fatty acids. *LWT Food Science and Technology*, *64*(2), 889–897.
Silveira, N., Longuinho, M. M., Leitão, S. G., Silva, R. S. F., Lourenço, M. C., Silva, P. E. A., & Finotelli, P. V. (2016). Synthesis and characterization of the antitubercular phenazine lapazine and development of PLGA and PCL nanoparticles for its entrapment. *Materials Science and Engineering: C*, *58*, 458–466.
Singh, C., Koduri, L. V. S. K., Dhawale, V., Bhatt, T. D., Kumar, R., Grover, V., & Suresh, S. (2015). Potential of aerosolized rifampicin lipospheres for modulation of pulmonary pharmacokinetics and bio-distribution. *International Journal of Pharmaceutics*, *495*(2), 627–632.
Singh, C., Koduri, L. V. S. K., Bhatt, T. D., Jhamb, S. S., Mishra, V., Gill, M. S., & Suresh, S. (2016). In vitro-in vivo evaluation of novel co-spray dried rifampicin phospholipid lipospheres for oral delivery. *AAPS PharmSciTech*, 1–9.
Sun, Y., Hu, Q., Qian, J., Li, T., Ma, P., Shi, D., & Chen, M. (2016). Preparation and properties of thermoplastic poly(caprolactone) composites containing high amount of esterified starch without plasticizer. *Carbohydrate Polymers*, *139*, 28–34.
Teodoro, A. P., Mali, S., Romero, N., & de Carvalho, G. M. (2015). Cassava starch films containing acetylated starch nanoparticles as reinforcement: Physical and mechanical characterization. *Carbohydrate Polymers*, *126*, 9–16.
Tewes, F., Brillault, J., Couet, W., & Olivier, J.-C. (2008). Formulation of rifampicin—Cyclodextrin complexes for lung nebulization. *Journal of Controlled Release*, *129*(2), 93–99.
Uchino, T., Tozuka, Y., Oguchi, T., & Yamamoto, K. (2002). Inclusion compound formation of amylose by sealed-heating with salicylic acid analogues. *Journal of Inclusion Phenomena and Macrocyclic Chemistry*, *43*(1-2), 31–36.
Wulff, G., Steinert, A., & Höller, O. (1998). Modification of amylose and investigation of its inclusion behavior. *Carbohydrate Research*, *307*(1–2), 19–31.
Wurzburg, O. B. (1964). Acetylation. *Methods in Carbohydrate Chemistry*, *4*, 286–288.
Yang, L., Zhang, B., Yi, J., Liang, J., Liu, Y., & Zhang, L. M. (2013). Preparation, characterization, and properties of amylose-ibuprofen inclusion complexes. *Starch Stärke*, *65*(7–8), 593–602.
Zaru, M., Sinico, C., De Logu, A., Caddeo, C., Lai, F., Manca, M. L., & Fadda, A. M. (2009). Rifampicin-loaded liposomes for the passive targeting to alveolar macrophages: In vitro and in vivo evaluation. *Journal of Liposome Research*, *19*(1), 68–76.
Zhang, L., Cheng, H., Zheng, C., Dong, F., Man, S., Dai, Y., & Yu, P. (2016). Structural and release properties of amylose inclusion complexes with ibuprofen. *Journal of Drug Delivery Science and Technology*, *31*, 101–107.
Zhou, Y., Li, X., Lv, Y., Shi, Y., Zeng, Y., Li, D., & Mu, C. (2016). Effect of oxidation level on the inclusion capacity and solution stability of oxidized amylose in aqueous solution. *Carbohydrate Polymers*, *138*, 41–48.